



Data Article

Comprehensive data compilation on the mechanical properties of refractory high-entropy alloys

J.-P. Couzinié ^{a,*}, O.N. Senkov ^b, D.B. Miracle ^b, G. Dirras ^c

^a Université Paris Est, ICMPE (UMR 7182) CNRS-UPEC, 2-8 rue Henri Dunant, 94320 Thiais, France

^b Air Force Research Laboratory, Materials and Manufacturing Directorate, Wright-Patterson AFB, OH 45433, USA

^c Université Paris 13, LSPM (UPR 3407) CNRS, 99 avenue J.B. Clément, 93430 Villetteuse, France

ARTICLE INFO

Article history:

Received 24 May 2018

Received in revised form

19 October 2018

Accepted 22 October 2018

ABSTRACT

This data article presents the compilation of mechanical properties for 122 refractory high entropy alloys (RHEAs) and refractory complex concentrated alloys (RCCAs) reported in the period from 2010 to the end of January 2018. The data sheet gives alloy composition, type of microstructures and the metallurgical states in which the properties are measured. Data such as the computed alloy mass density, the type of mechanical loadings to which they are subjected and the corresponding macroscopic mechanical properties, such as the yield stress, are made available as a function of the testing temperature. For practical use, the data are tabulated and some are also graphically presented, allowing at a glance to access relevant information for this attractive category of RHEAs and RCCAs.

© 2018 The Authors. Published by Elsevier Inc. This is an open access article under the CC BY license (<http://creativecommons.org/licenses/by/4.0/>).

Specifications table

Subject area	Materials Science
More specific subject area	<i>Refractory high-entropy alloys (RHEAs) and refractory complex concentrated alloys (RCCAs)</i>

* Corresponding author.

E-mail address: couzinie@icmpe.cnrs.fr (J.-P. Couzinié).

Type of data	Table, figures
How data was acquired	Compilation of data from available literature. Data extracted from studies on 122 alloys reported in the period from 2010 to January 2018
Data format	Analyzed
Experimental factors	Data compilation from available literature. Data sheet contains about 54 references.
Experimental Features	Extensive Data compilation. Alloys' mass densities and Young modulus were computed using the rule of mixtures (ROM) for the different reported alloy compositions.
Data source location	From the literature, as well as the authors' calculations. References are given in the corresponding sections.
Data accessibility	Data are with the article
Related research article	Direct submission. Most relevant research article: Senkov, Oleg; Miracle, Daniel; Chaput, Kevin; Couzinie, Jean-Philippe, <i>Development and Exploration of Refractory High Entropy Alloys – A Review</i> , <i>Journal of Materials Research</i> , 33 (19), (2018), 3092–3128, https://doi.org/10.1557/jmr.2018.153 [1]

Value of the data

- The comprehensive data compilation provides up-to-date mechanical properties of RHEAs and RCCAs tested under uniaxial loading on the basis of published reports from 2010 through the end of January 2018.
- The dataset contains pertinent references, readily accessible to all researchers.
- Processed data may be used to evaluate the potential of RHEAs and RCCAs as possible structural materials.
- The data compilation can be used as a primary tool and as a guidance for further development of RHEAs and RCCAs.
- This data compilation can enable machine learning and data analytics methods to extract insights and trends not available from individual studies, thus accelerating the development of these alloys.

1. Data

Refractory High Entropy Alloys (RHEAs) and Refractory Complex Concentrated Alloys (RCCAs) are attractive materials and promising candidates for structural high temperature applications. Deriving from a new alloying design strategy, RHEAs contain five or more elements with concentration between 5 and 35 at% and RCCAs expand this vast range of new alloys even further by including three or more principal elements and expanding the concentrations of these elements beyond 35% [1]. Further, RHEAs are sometimes considered to be only single-phase, disordered solid solution alloys, while RCCAs can have any number of phases and can also include ordered, intermetallic phases. The presented database is a compilation of the mechanical properties of RHEAs and RCCAs from a large number of studies published during the 2010–January 2018 period. Each row in Table 1 corresponds to one mechanical test for an alloy composition in an experimentally characterized metallurgical condition. The data are gathered in a table compiling all the published results such that it could be graphically represented and analyzed afterward [2]. The table also provides the alloy densities calculated in this work using rule of mixtures (ROM), as well as Young's moduli for single-phase alloys calculated using ROM.

2. Experimental design, materials, and methods

The presented data sheet is a compilation of essential data on RHEAs and RCCAs. All RHEAs and RCCAs reported in the literature through the end of January 2018 crystallize with at least one phase

Table 1

RHEAs and RCCAs for which mechanical tests are reported in literature. Each line represents the result of a test on a specific alloy composition. The experimental Young modulus is given in brackets in the adequate column. Values appearing in brackets in the yield strength column correspond to the fracture stress without plastic deformation See text for explanations [57–60].

Composition (mole fraction)	Ref.	ρ (g.cm ⁻³) ROM	Young modulus (GPa) ROM	Young Modulus (GPa) (experimental) /first principles	Equilibrium conditions	Single/ Multiphase material	Type of present phases	Tension/ Compre- sion	Testing T (°C)	σ_Y (MPa)	σ_Y/ρ (MPa.cm ³ .g ⁻¹)
Al0.25MoNbTiV	[3]	7.1	163.6	168.0 [57]	AC	S	BCC	C	RT	1250	176.9
Al0.25NbTaTiV	[4]	8.8	130.0	(94.0)	AC	S	BCC	C	RT	1330	151.2
Al0.25NbTaTiZr	[5]	8.6		(118.0)	HIP+A	M	BCC+B2	C	RT	1745	203.1
Al0.25NbTaTiZr	[5]	8.6		(63.0)	HIP+A	M	BCC+B2	C	1000	366	42.6
Al0.2MoTaTiV	[6]	9.3	184.0		AC	S	BCC	C	RT	1021	110.3
Al0.3HfNbTaTiZr	[7]	9.6	108.3	(63.0)	AC	S	BCC	C	RT	1188	124.4
Al0.3NbTa0.8Ti1.4V0.2Zr1.3	[8]	7.7	110.2		HIP+A	S	BCC	C	RT	1965	255.0
Al0.3NbTa0.8Ti1.4V0.2Zr1.3	[8]	7.7			HIP+A	S	BCC	C	1000	166	21.5
Al0.3NbTa0.8Ti1.4V0.2Zr1.3	[8]	7.7			HIP+A	S	BCC	C	800	678	88.0
Al0.3NbTaTi1.4Zr1.3	[8]	8.1			HIP+A	M	BCC+B2	C	RT	1965	242.9
Al0.3NbTaTi1.4Zr1.3	[8]	8.1			HIP+A	M	BCC+B2	C	1000	236	29.2
Al0.3NbTaTi1.4Zr1.3	[8]	8.1			HIP+A	M	BCC+B2	C	800	362	44.7
Al0.4Hf0.6NbTaTiZr	[8]	9.1	110.0		HIP+A	S	BCC	C	RT	1841	202.5
Al0.4Hf0.6NbTaTiZr	[8]	9.1			HIP+A	S	BCC	C	1000	298	32.8
Al0.4Hf0.6NbTaTiZr	[8]	9.1			HIP+A	S	BCC	C	800	796	87.6
Al0.4Hf0.6NbTaTiZr	[9]	9.1	110.0	(78.1)	HIP+A	S	BCC	C	RT	1841	202.5
Al0.4Hf0.6NbTaTiZr	[9]	9.1			HIP+A	S	BCC	C	1200	89	9.8

Al0.4Hf0.5Nb1Ta1Zr	[9]	9.1		(23.3)	Hf+Al	S	BCC	C	1000	298	32.8
Al0.4Hf0.5Nb1Ta1Zr	[9]	9.1		(48.8)	Hf+Al	S	BCC	C	800	796	87.6
Al0.5CrNbTi2V0.5	[10]	5.8		A	M	BCC+Laves	C	RT	1340		232.4
Al0.5CrNbTi2V0.5	[10]	5.8	143.0	AC	S	BCC	C	RT	1240		215.0
Al0.5CrNbTi2V0.5	[10]	5.8		A	M	BCC+Laves	C	1000	90		15.6
Al0.5CrNbTi2V0.5	[10]	5.8		A	M	BCC+Laves	C	800	445		77.2
Al0.5CrNbTi2V0.5	[10]	5.8		A	M	BCC+Laves	C	600	930		161.3
Al0.5HfNb1Ta1Zr	[7]	9.3	106.9	(97.0)	AC	S	BCC	C	RT	1302	139.4
Al0.5Mo0.5Nb1Ta0.5Ti2Zr	[5]	7.6		(132.0)	Hf+Al	M	BCC+B2	C	RT	2350	309.7
Al0.5Mo0.5Nb1Ta0.5Ti2Zr	[5]	7.6		(78.0)	Hf+Al	M	BCC+B2	C	1000	579	76.3
Al0.5MoNb1TV	[3]	6.8	158.4	172.1[57]	AC	S	BCC	C	RT	1625	238.3
Al0.5NbTa0.8Ti1.5V0.2Zr	[8]	7.6	111.3		Hf+Al	M	BCC+B2	C	RT	2035	259.2
Al0.5NbTa0.8Ti1.5V0.2Zr	[8]	7.6			Hf+Al	M	BCC+B2	C	1000	220	29.1
Al0.5NbTa0.8Ti1.5V0.2Zr	[8]	7.6			Hf+Al	M	BCC+B2	C	800	796	105.3
Al0.5NbTa1TV	[4]	8.5	126.7	(98.0)	AC	S	BCC	C	RT	1012	119.6
Al0.5Mo1Ta1TV	[6]	8.7	174.1		AC	S	BCC	C	RT	962	110.9
Al0.75Nb1Ta1Zr	[7]	9.1	105.3	(102.0)	AC	S	BCC	C	RT	1415	155.6
Al0.75Nb1Ta1TV	[3]	6.6	153.8	173.9[57]	AC	S	BCC	C	RT	1260	191.0
Al1.5MoNb1TV	[3]	6.1	142.4	173.8[57]	AC	S	BCC	C	RT	500	82.5
AlCr0.5Nb1TV	[11]	5.6	124.1		A	S	BCC	C	RT	1300	230.6
AlCr0.5Nb1TV	[11]	5.6			A	S	BCC	C	1000	40	7.1
AlCr0.5Nb1TV	[11]	5.6			A	S	BCC	C	800	640	113.5
AlCr0.5Nb1TV	[11]	5.6			A	S	BCC	C	600	1005	178.2
AlCr1.5Nb1TV	[11]	5.9			A	M	BCC+Laves	C	RT	1700	290.1
AlCr1.5Nb1TV	[11]	5.9			A	M	BCC+Laves	C	1000	75	12.8
AlCr1.5Nb1TV	[11]	5.9			A	M	BCC+Laves	C	800	970	165.5
AlCr1.5Nb1TV	[11]	5.9			A	M	BCC+Laves	C	600	1370	233.8
AlCrNbMnTi	[12]	6.6			A	M	BCC+Unknown	C	RT	(1010)	-
AlCrNbMnTi	[12]	6.6			A	M	BCC+Unknown	C	1200	105	16.0
AlCrNbMnTi	[12]	6.6			A	M	BCC+Unknown	C	1000	594	90.5

AlCrMnO ₃	[12]	6.6		A	M	BCC+Unknown	C	800	860	131.0
AlCrMnO ₃	[12]	6.6		A	M	BCC+Unknown	C	600	1060	161.4
AlCrMnO ₃	[12]	6.6		A	M	BCC+Unknown	C	400	1080	164.5
AlCrMnO ₃	[13]	6.6		A	S	BCC	C	1200	150	22.8
AlCrMnO ₃	[13]	6.6		A	S	BCC	C	1000	550	83.8
AlCrMnO ₃	[13]	6.6		A	S	BCC	C	800	875	133.2
AlCrMnO ₃	[13]	6.6		A	S	BCC	C	600	930	141.6
AlCrMo ₃	[13]	6.0		A	S	BCC	C	1200	100	16.7
AlCrMo ₃	[13]	6.0		A	S	BCC	C	1000	375	62.7
AlCrMo ₃	[13]	6.0		A	S	BCC	C	800	875	146.3
AlCrMo ₃	[13]	6.0		A	S	BCC	C	600	1020	170.5
AlCrNb ₃ Ti ₂ V	[14]	5.8		A	S	BCC+Laves	C	400	1070	178.9
AlCrNb ₃ Ti ₂ V	[14]	5.8		A	M	BCC+Laves	C	RT	1550	259.2
AlCrNb ₃ Ti ₂ V	[14]	5.8		A	M	BCC+Laves	C	1000	65	11.3
AlCrNb ₃ Ti ₂ V	[14]	5.8		A	M	BCC+Laves	C	800	860	149.4
AlCrNb ₃ Ti ₂ V	[14]	5.8		A	M	BCC+Laves	C	600	1015	176.3
AlHfNb ₃ Ta ₂ Zr	[7]	8.9	(103.0)	AC	M	2BCC	C	RT	1489	168.0
AlMo _{0.5} Nb ₁ Ta _{0.5} Tzr	[5]	7.1	(122.0)	HIP+A	M	BCC+B2	C	RT	2197	307.4
AlMo _{0.5} Nb ₁ Ta _{0.5} Tzr	[5]	7.1	(70.0)	HIP+A	M	BCC+B2	C	1000	745	104.2
AlMo _{0.5} Nb ₁ Ta _{0.5} Tzr	[8]	7.1		HIP+A	M	BCC+B2	C	RT	2000	279.8
AlMo _{0.5} Nb ₁ Ta _{0.5} Tzr	[8]	7.1		HIP+A	M	BCC+B2	C	1000	745	104.2
AlMo _{0.5} Nb ₁ Ta _{0.5} Tzr	[8]	7.1		HIP+A	M	BCC+B2	C	800	1597	223.4
AlMo _{0.5} Nb ₁ Ta _{0.5} Tzr	[9]	7.1	(178.6)	HIP+A	M	BCC+B2	C	RT	2000	279.8
AlMo _{0.5} Nb ₁ Ta _{0.5} Tzr	[9]	7.1	(27.0)	HIP+A	M	BCC+B2	C	1200	250	35.0
AlMo _{0.5} Nb ₁ Ta _{0.5} Tzr	[9]	7.1	(36.0)	HIP+A	M	BCC+B2	C	1000	745	104.2
AlMo _{0.5} Nb ₁ Ta _{0.5} Tzr	[9]	7.1	(80.0)	HIP+A	M	BCC+B2	C	800	1597	223.4
AlMo _{0.5} Nb ₁ Ta _{0.5} Tzr	[14]	7.1		HIP+A	M	BCC+B2	C	RT	2000	279.8
AlMo _{0.5} Nb ₁ Ta _{0.5} Tzr	[14]	7.1		HIP+A	M	BCC+B2	C	1200	250	35.0
AlMo _{0.5} Nb ₁ Ta _{0.5} Tzr	[14]	7.1		HIP+A	M	BCC+B2	C	1000	745	104.2
AlMo _{0.5} Nb ₁ Ta _{0.5} Tzr	[14]	7.1		HIP+A	M	BCC+B2	C	800	1597	223.4

AlNbC0.5NbTa0.5TiZr	[14]	7.1		HIP+A	M	BCC+B2	C	600	1870	231.6	
AlNbC0.5NbTa0.5TiZr0.5	[5]	7.2	(133.0)	HIP+A	S	B2	C	RT	(1320)	-	
AlNbC0.5NbTa0.5TiZr0.5	[5]	7.2	(76.0)	HIP+A	S	B2	C	1000	935	139.1	
AlNbNbTi	[13]	6.5	A	S	BCC	C	1200	200	31.0		
AlNbNbTi	[13]	6.5	A	S	BCC	C	1000	540	83.6		
AlNbNbTi	[13]	6.5	A	S	BCC	C	800	500	77.4		
AlNbNbTi	[13]	6.5	A	S	BCC	C	600	520	80.5		
AlNbNbTiV	[3]	6.4	149.6	174.4 [57]/285.4 [58]	AC	S	BCC	C	RT	1375	214.9
AlNbNbTiV	[6]	8.2	165.8	AC	S	BCC	C	RT	(735)	-	
AlNb1.5Ta0.5Ti1.5Zr0.5	[8]	6.8	105.7	HIP+A	S	BCC	C	RT	1280	186.9	
AlNb1.5Ta0.5Ti1.5Zr0.5	[8]	6.8	HIP+A	S	BCC	C	1000	403	58.8		
AlNb1.5Ta0.5Ti1.5Zr0.5	[8]	6.8	HIP+A	S	BCC	C	800	728	106.3		
AlNbTa0.5TiZr0.5	[5]	6.9	(124.0)	HIP+A	S	B2	C	RT	1352	195.3	
AlNbTa0.5TiZr0.5	[5]	6.9	(53.0)	HIP+A	S	B2	C	1000	535	77.3	
AlNbTaTiV	[4]	7.9	121.0	AC	S	BCC	C	RT	991	125.6	
AlNbTiV	[11]	5.5	104.8	A	S	BCC	C	RT	1000	181.9	
AlNbTiV	[11]	5.5	A	S	BCC	C	1000	110	20.0		
AlNbTiV	[11]	5.5	A	S	BCC	C	800	560	101.9		
AlNbTiV	[11]	5.5	A	S	BCC	C	600	780	141.9		
AlNbTiV	[15]	5.5	104.8	A	S	BCC	C	RT	1020	195.6	
AlNbTiV	[15]	5.5	A	S	BCC	C	1000	158	28.7		
AlNbTiV	[15]	5.5	A	S	BCC	C	800	685	124.6		
AlNbTiV	[15]	5.5	A	S	BCC	C	600	810	147.4		
AlNbTiV	[16]	5.5	A	S	B2	C	RT	1000	181.9		
AlNbTiV	[16]	5.5	A	S	B2	C	800	560	101.9		
AlNbTiV	[16]	5.5	A	S	B2	C	600	780	141.9		
AlNbTiZr	[16]	5.8	A	M	B2+A3Zr5+Laves	C	RT	1500	260.4		
AlNbTiZr	[16]	5.8	A	M	B2+A3Zr5+Laves	C	800	550	95.5		
AlNbTiZr	[16]	5.8	A	M	B2+A3Zr5+Laves	C	600	1155	200.5		

AlNbTiZrO ₁	[16]	5.5		A	M	B2+Al3Zr5	C	RT	1290	233.2
AlNbTiZrO _{1.1}	[16]	5.5		A	M	B2+Al3Zr5	C	800	865	156.4
AlNbTiZrO _{1.1}	[16]	5.5		A	M	B2+Al3Zr5	C	600	975	176.3
AlNbTiZrO _{2.5}	[16]	5.6		A	M	B2+Al3Zr5	C	RT	1360	243.8
AlNbTiZrO _{2.5}	[16]	5.6		A	M	B2+Al3Zr5	C	800	855	153.3
AlNbTiZrO _{2.5}	[16]	5.6		A	M	B2+Al3Zr5	C	600	1065	190.9
AlNbTiZrO ₅	[16]	5.6		A	M	B2+Al3Zr5+Laves	C	RT	1485	262.9
AlNbTiZrO ₅	[16]	5.6		A	M	B2+Al3Zr5+Laves	C	800	675	119.5
AlNbTiZrO ₅	[16]	5.6		A	M	B2+Al3Zr5+Laves	C	600	1135	200.9
AlNbTiZrO _{1.5}	[16]	5.8		A	M	B2+Al3Zr5+Laves	C	RT	1535	252.6
AlNbTiZrO _{1.5}	[16]	5.8		A	M	B2+Al3Zr5+Laves	C	800	180	30.8
AlNbTiZrO _{1.5}	[16]	5.8		A	M	B2+Al3Zr5+Laves	C	600	(1195)	204.4
Co ₁ Hf _{0.5} Mn _{0.5} Nb ₁ Zr	[17]	7.8		AC	M	BCC+MC	C	RT	1183	151.5
Co ₃ Hf _{0.5} Mn _{0.5} Nb ₁ Zr	[17]	7.7		AC	M	BCC+MC	C	RT	1201	156.2
CoCrMnNb	[18]	8.8		AC	M	BCC+Laves	C	RT	(1419.6)	-
CoCrMnNbTi	[18]	7.8		AC	M	BCC+Laves	C	RT	(1096.8)	-
CoCrMnNbTiO ₂	[18]	8.5		AC	M	BCC+Laves	C	RT	(1905.6)	-
CoCrMnNbTiO ₄	[18]	8.3	220.1	AC	S	BCC	C	RT	(1717.3)	-
CoCrMnNbTiO ₅	[18]	8.2		AC	M	BCC+Laves	C	RT	(1609.2)	-
CrHfNbTiZr	[19]	8.2		(112.0)	A	BCC+Laves	C	RT	1457	176.9
CrHfNbTiZr	[19]	8.2		(112.0)	A	BCC+Laves	C	RT	1420	172.4
CrHfNbTiZr	[19]	8.2		(112.0)	AC	BCC+Laves	C	RT	1375	167.0
CrHfNbTiZr	[19]	8.2		(112.0)	A	BCC+Laves	C	RT	1328	161.3
CrHfNbTiZr	[19]	8.2		(112.0)	A	BCC+Laves	C	RT	1322	160.5
CrMo _{0.5} Nb ₁ Ta _{0.5} TiZr	[20]	8.0		Hf+TA	M	2BCC+Laves	C	RT	1595	199.5
CrMo _{0.5} Nb ₁ Ta _{0.5} TiZr	[20]	8.0		Hf+TA	M	2BCC+Laves	C	1200	170	21.3
CrMo _{0.5} Nb ₁ Ta _{0.5} TiZr	[20]	8.0		Hf+TA	M	2BCC+Laves	C	1000	546	68.3
CrMo _{0.5} Nb ₁ Ta _{0.5} TiZr	[20]	8.0		Hf+TA	M	2BCC+Laves	C	800	983	122.9
CrNbTiZr	[21]	6.6		Hf+TA	M	BCC+Laves	C	RT	1298	197.8
CrNbTiZr	[21]	6.6		Hf+TA	M	BCC+Laves	C	1000	259	39.5

CrNbTiZr	[21]	6.6		Hf+IA	M	BCC+Laves	C	800	615	93.7	
CrNbTiZr	[21]	6.6		Hf+IA	M	BCC+Laves	C	600	1230	187.4	
CrNbTiZr	[21]	6.6		Hf+IA	M	BCC+Laves	C	RT	1260	189.5	
CrNbTiZr	[21]	6.6		Hf+IA	M	BCC+Laves	C	1000	115	17.3	
CrNbTiZr	[21]	6.6		Hf+IA	M	BCC+Laves	C	800	300	45.1	
CrNbTiZr	[21]	6.6		Hf+IA	M	BCC+Laves	C	600	1035	155.7	
CrTaTi0.7W	[22]	12.6		SPS	M	BCC+Laves	C	RT	2034	161.0	
CrTaTi0.7W	[22]	12.6		SPS	M	BCC+Laves	C	1200	750	59.4	
CrTaTi0.3VW	[22]	12.3		SPS	M	BCC+Laves	C	RT	2050	166.1	
CrTaTi0.3VW	[22]	12.3		SPS	M	BCC+Laves	C	1200	586	47.5	
CrTaVW	[22]	13.0		SPS	M	BCC+Laves	C	RT	2327	178.5	
CrTaVW	[22]	13.0		SPS	M	BCC+Laves	C	1200	979	75.1	
Hf0.4Nb1.5Ta1.54Ti0.89Zr0.64	[23]	10.4	125.0	(79.0)	AC	S	BCC	C	RT	822	79.1
Hf0.4Nb1.5Ta1.54Ti0.89Zr0.64	[23]	10.4		AC	S	BCC	C	300	590	56.8	
Hf0.4Nb1.5Ta1.54Ti0.89Zr0.64	[23]	10.4		AC	S	BCC	C	200	650	62.6	
Hf0.4Nb1.5Ta1.54Ti0.89Zr0.64	[23]	10.4		AC	S	BCC	C	100	765	73.7	
Hf0.4Nb1.5Ta1.54Ti0.89Zr0.64	[23]	10.4		AC	S	BCC	C	60	795	76.5	
Hf0.5Nb0.5NbSi0.1TiZr	[24]	7.7		AC	M	BCC+M5S3	C	RT	1350	174.6	
Hf0.5Nb0.5NbSi0.3TiZr	[24]	7.5		AC	M	BCC+M5S3	C	RT	1370	183.3	
Hf0.5Nb0.5NbSi0.5TiZr	[24]	7.2		AC	M	BCC+M5S3	C	RT	1600	221.0	
Hf0.5Nb0.5NbSi0.7TiZr	[24]	7.0		AC	M	BCC+M5S3	C	RT	1550	220.6	
Hf0.5Nb0.5NbSi0.9TiZr	[24]	6.8		AC	M	BCC+M5S3	C	RT	1650	241.5	
Hf0.5Nb0.5NbTiZr	[17]	7.9	123.1	AC	S	BCC	C	RT	1176	149.4	
Hf0.5Nb0.5NbTiZr	[24]	7.9	123.1	AC	S	BCC	C	RT	1150	146.1	
Hf0.5Nb0.5Ta0.5Ti1.25	[25]	8.2	106.6	AC	S	BCC	C	RT	903	110.3	
Hf0.5Nb0.5NbTa0.5Ti1.25	[25]	8.4	103.1	(78.0)	CR	S	BCC	C	RT	1150	136.7
Hf0.5Nb0.5NbTa0.5Ti1.25	[26]	8.4	103.1	(78.0)	CR	S	BCC	C	RT	1100	130.8
Hf0.5Nb0.5NbTa0.5Ti1.25	[26]	8.4	103.1	(80.0)	Cr+A	S	BCC	C	RT	890	105.8
Hf0.75NbTa0.5Ti1.25	[26]	8.4	103.1	(78.0)	CR	S	BCC	C	72	1040	123.7
Hf0.75NbTa0.5Ti1.25	[26]	8.4	103.1	(78.0)	CR	S	BCC	C	72	1020	121.3

Hf0.75NbTa0.5Tl1.5Zr1.25	[26]	8.4		(80.0)	CR+A	S	BCC	C	72	640	76.1
Hf0.75NbTa0.5Tl1.5Zr1.25	[26]	8.4		(78.0)	CR	S	BCC	C	-43	1200	142.7
Hf0.75NbTa0.5Tl1.5Zr1.25	[26]	8.4		(78.0)	CR	S	BCC	C	-43	1180	140.3
Hf0.75NbTa0.5Tl1.5Zr1.25	[26]	8.4		(80.0)	CR+A	S	BCC	C	-43	1020	121.3
Hf0.75NbTa0.5Tl1.5Zr1.25	[26]	8.4		(78.0)	CR	S	BCC	C	-103	1380	164.1
Hf0.75NbTa0.5Tl1.5Zr1.25	[26]	8.4		(78.0)	CR	S	BCC	C	-103	1370	162.9
Hf0.75NbTa0.5Tl1.5Zr1.25	[26]	8.4		(80.0)	CR+A	S	BCC	C	-103	1250	148.6
Hf0.75NbTa0.5Tl1.5Zr1.25	[26]	8.4		(78.0)	CR	S	BCC	C	-153	1640	195.0
Hf0.75NbTa0.5Tl1.5Zr1.25	[26]	8.4		(78.0)	CR	S	BCC	C	-153	1550	184.3
Hf0.75NbTa0.5Tl1.5Zr1.25	[26]	8.4		(80.0)	CR+A	S	BCC	C	-153	1370	162.9
Hf0.75NbTa0.5Tl1.5Zr1.25	[26]	8.4		(80.0)	CR+A	S	BCC	C	-196	1320	288.3
Hf0.75NbTa0.5Tl1.5Zr1.25	[26]	8.4		(78.0)	CR	S	BCC	C	-196	1380	233.5
Hf0.75NbTa0.5Tl1.5Zr1.25	[26]	8.4		(78.0)	CR	S	BCC	C	-196	1750	288.1
Hf0.75NbTa0.5Tl1.5Zr1.25	[26]	8.4		(80.0)	CR+A	S	BCC	C	-268.8	2390	284.2
Hf0.75NbTa0.5Tl1.5Zr1.25	[26]	8.4		(78.0)	CR	S	BCC	C	-268.8	2250	267.5
Hf0.75NbTa0.5Tl1.5Zr1.25	[26]	8.4		(78.0)	CR	S	BCC	C	-268.8	2210	262.8
HfMo0.25Nb0.75Ta0.5	[27]	9.9	121.0	(96.0)	AC	S	BCC	C	RT	1112	112.2
HfMo0.5Nb0.5Ta0.5	[28]	8.5			AC	M	BCC+M5S3	C	RT	1617	191.0
HfMo0.5Nb0.5Ta0.5	[28]	8.5			AC	M	BCC+M5S3	C	1200	166	19.6
HfMo0.5Nb0.5Ta0.5	[28]	8.5			AC	M	BCC+M5S3	C	1000	398	47.0
HfMo0.5Nb0.5Ta0.5	[28]	8.2			AC	M	BCC+M5S3	C	RT	1787	218.7
HfMo0.5Nb0.5Ta0.5	[28]	8.2			AC	M	BCC+M5S3	C	1200	188	23.0
HfMo0.5Nb0.5Ta0.5	[28]	8.2			AC	M	BCC+M5S3	C	1000	614	75.2
HfMo0.5Nb0.5Ta0.5	[28]	7.9			AC	M	BCC+M5S3	C	RT	2134	270.1
HfMo0.5Nb0.5Ta0.5	[28]	7.9			AC	M	BCC+M5S3	C	1200	235	29.7
HfMo0.5Nb0.5Ta0.5	[28]	7.9			AC	M	BCC+M5S3	C	1000	673	85.2
HfMo0.5Nb0.5Ta0.5	[27]	9.9	130.5	(102.0)	AC	S	BCC	C	RT	1317	132.8
HfMo0.5Nb0.5Ta0.5	[28]	9.0	131.9		AC	S	BCC	C	RT	1260	140.4
HfMo0.5Nb0.5Ta0.5	[28]	9.0			AC	S	BCC	C	1200	60	6.7
HfMo0.5Nb0.5Ta0.5	[28]	9.0			AC	S	BCC	C	1000	368	41.0

HfMoO _{0.75} Nb _{0.1} Ti _{0.12} r	[27]	9.9	139.1	(109.0)	AC	S	BCC	C	RT	1373	138.3
HfMoNb _{0.1} Ta _{0.1} Ti _{0.12} r	[27]	9.9	147.0	(115)/[36.6 [58]]	AC	S	BCC	C	RT	1512	152.1
HfMoNb _{0.1} Ta _{0.1} Ti _{0.12} r	[29]	9.9	147.0	136.6 [58]	AC	S	BCC	C	RT	1512	152.1
HfMoNb _{0.1} Ta _{0.1} Ti _{0.12} r	[29]	9.9			AC	S	BCC	C	1200	556	55.9
HfMoNb _{0.1} Ta _{0.1} Ti _{0.12} r	[29]	9.9			AC	S	BCC	C	1000	814	81.9
HfMoNb _{0.1} Ta _{0.1} Ti _{0.12} r	[29]	9.9			AC	S	BCC	C	800	1007	101.3
HfMoNb _{0.1} Ti _{0.12} r	[30]	8.7	139.2		AC	S	BCC	C	RT	1219	197.9
HfMoNb _{0.1} Ti _{0.12} r	[30]	8.7	139.2	A	S	BCC	C	RT	1575	181.3	
HfMoNb _{0.1} Ti _{0.12} r	[30]	8.7		AC	S	BCC	C	1200	187	21.5	
HfMoNb _{0.1} Ti _{0.12} r	[30]	8.7		AC	S	BCC	C	1100	397	45.7	
HfMoNb _{0.1} Ti _{0.12} r	[30]	8.7		AC	S	BCC	C	1000	635	73.1	
HfMoNb _{0.1} Ti _{0.12} r	[30]	8.7		AC	S	BCC	C	900	728	83.8	
HfMoNb _{0.1} Ti _{0.12} r	[30]	8.7		AC	S	BCC	C	800	825	95.0	
HfMoTa _{0.1} Ti _{0.12} r	[29]	10.2	155.4		AC	S	BCC	C	RT	1600	157.0
HfMoTa _{0.1} Ti _{0.12} r	[29]	10.2		AC	S	BCC	C	1200	404	39.6	
HfMoTa _{0.1} Ti _{0.12} r	[29]	10.2		AC	S	BCC	C	1000	855	83.9	
HfMoTa _{0.1} Ti _{0.12} r	[29]	10.2		AC	S	BCC	C	800	1045	102.5	
HfNb _{0.18} Ta _{0.12} Ti _{1.27} r	[31]	8.5	95.2	(79.0)	Cr+A	S	BCC	T	RT	540	63.8
HfNb _{0.3} Ti _{0.1} V	[32]	7.8		AC	M	BCC+M5S3	C	RT	1399	179.3	
HfNb _{0.3} Ti _{0.1} V	[32]	7.8		AC	M	BCC+M5S3	C	1000	240	30.8	
HfNb _{0.3} Ti _{0.1} V	[33]	7.8		AC	M	BCC+M5S3	C	800	875	112.2	
HfNb _{0.3} Ti _{0.1} V	[33]	7.5		AC	M	BCC+Laves+M5S3	C	RT	1540	204.9	
HfNb _{0.3} Ti _{0.1} V	[33]	7.5		A	M	BCC+Laves+M5S3	C	RT	1483	197.4	
HfNb _{0.3} Ti _{0.1} V	[33]	7.5		AC	M	BCC+Laves+M5S3	C	800	371	49.4	
HfNb _{0.3} Ti _{0.1} V	[33]	7.5		A	M	BCC+Laves+M5S3	C	800	102	13.6	
HfNb _{0.3} Ti _{0.1} V	[33]	7.5		AC	M	BCC+Laves+M5S3	C	600	920	122.4	
HfNb _{0.3} Ti _{0.1} V	[33]	7.5		A	M	BCC+Laves+M5S3	C	600	597	79.4	
HfNb _{0.3} Ti _{0.1} V	[33]	7.5		A	M	BCC+Laves+M5S3	C	400	1273	169.4	
HfNbTa _{0.1} Ti _{0.12} r	[7]	9.9	110.6	(55)/88.9 [58]/104.1[19]	AC	S	BCC	C	RT	1073	108.4

HNB-TATZ-	[27]	9.9	110.6	[85]/[88.9]	AC	S	BCC	C	RT	1015	102.6
HNB-TATZ-	[34]	9.9	110.6	[58]/[104.1][19]	SPD+IA	M	BCC+HCP	T	RT	1520	133.6
HNB-TATZ-	[34]	9.9	110.6	[58]/[104.1][19]	SPD+IA	M	2 BCC+HCP	T	RT	795	80.4
HNB-TATZ-	[34]	9.9	110.6	[58]/[104.1][19]	SPD	S	BCC	T	RT	1900	192.0
HNB-TATZ-	[34]	9.9	110.6	[58]/[104.1][19]	CR+A	S	BCC	T	RT	830	83.9
HNB-TATZ-	[35]	9.9	110.6	[100.0]	CR+A	M	2 BCC	T	RT	1303	131.7
HNB-TATZ-	[35]	9.9	110.6	[58]/[88.9]	CR	S	BCC	T	RT	1202	121.5
HNB-TATZ-	[35]	9.9	110.6	[58]/[104.1][19]	CR+A	S	BCC	T	RT	1145	115.7
HNB-TATZ-	[36]	9.9	110.6	[58]/[104.1][19]	CR+A	S	BCC	T	RT	958	96.8
HNB-TATZ-	[36]	9.9	110.6	[58]/[104.1][19]	CR+A	S	BCC	T	RT	944	95.4
HNB-TATZ-	[36]	9.9	110.6	[58]/[88.9]	CR+A	S	BCC	T	RT	940	95.0
HNB-TATZ-	[37]	9.9	110.6	[58]/[104.1][19]	CR+A	S	BCC	T	RT	940	95.0
HNB-TATZ-	[38]	9.9	110.6	[58]/[104.1][19]	HIP+IA	S	BCC	C	RT	929	93.9
HNB-TATZ-	[39]	9.9	110.6	[58]/[104.1][19]	AC	S	BCC	C	RT	905	91.5
HNB-TATZ-	[40]	9.9	110.6	[58]/[104.1][19]	AC	S	BCC	C	RT	890	90.0
HNB-TATZ-	[41]	9.9	110.6	[58]/[104.1][19]	AC	S	BCC	T	RT	828	83.7
HNB-TATZ-	[41]	9.9	110.6	[58]/[104.1][19]	AC	S	BCC	T	RT	827	83.6
HNB-TATZ-	[41]	9.9	110.6	[58]/[104.1][19]	AC	S	BCC	T	RT	820	82.9
HNB-TATZ-	[41]	9.9	110.6	[58]/[104.1][19]	AC	S	BCC	T	RT	803	81.2
HNB-TATZ-	[42]	9.9		[58]/[104.1][19]	HIP+IA	S	BCC	C	1200	92	9.3
HNB-TATZ-	[42]	9.9			HIP+IA	S	BCC	C	1000	295	29.8
HNB-TATZ-	[42]	9.9			HIP+IA	S	BCC	C	800	535	54.1
HNB-TATZ-	[42]	9.9			HIP+IA	S	BCC	C	800	475	48.0
HNB-TATZ-	[42]	9.9			HIP+IA	S	BCC	C	800	285	28.8
HNB-TATZ-	[42]	9.9			HIP+IA	S	BCC	C	600	675	68.2

HNbTaTzr	[42]	9.9		HIP+IA	S	BCC	C	400	790	79.8	
HNbTaZr	[43]	11.1		A	M	BCC+HCP	C	RT	2310	208.8	
HNbTaZr	[43]	11.1		A	M	BCC+HCP	C	RT	2100	139.8	
HNbTaZr	[43]	11.1		A	M	BCC+HCP	C	RT	2020	132.6	
HNbTaZr	[43]	11.1		A	M	BCC+HCP	C	RT	1950	176.3	
HNbTaZr	[43]	11.1	109.3	AC	S	BCC	C	RT	1315	118.9	
HNbTaTzr	[19]	8.1	(128.0)	A	M	BCC+Laves	C	RT	1157	143.5	
HNbTaTzr	[19]	8.1	(128.0)	AC	M	BCC+Unknown	C	RT	1170	145.2	
HNbTaTzr	[19]	8.1	99.0	(128.0)95.0	A	BCC	C	RT	1253	155.5	
HNbTaTzr	[19]	8.1	99.0	(128.0)95.0	A	S	BCC	C	RT	1140	141.4
HNbTaTzr	[19]	8.1	99.0	(128.0)95.0	A	S	BCC	C	RT	1120	139.0
HNbTaTzr	[44]	8.4	91.8	A	S	BCC	T	RT	879	104.8	
HfTa0.4Tzr	[45]	9.2		AC	M	BCC+HCP	T	RT	400	43.5	
HfTa0.5Tzr	[45]	9.4		AC	M	BCC+HCP	T	RT	700	74.7	
HfTa0.6Tzr	[45]	9.6		AC	M	BCC+HCP	T	RT	800	83.7	
HfTaTzr	[45]	10.2	112.0	AC	S	BCC	T	RT	1500	147.3	
Mo0.1NbTv0.32r	[46]	6.6	106.0	AC	S	BCC	C	RT	932	141.2	
Mo0.3NbTv0.32r	[46]	6.8	118.4	AC	S	BCC	C	RT	1312	133.9	
Mo0.3NbTvZr	[46]	6.7	119.9	AC	S	BCC	C	RT	1289	132.8	
Mo0.5NbTv0.32r	[46]	6.9	129.4	AC	S	BCC	C	RT	1301	138.0	
Mo0.5NbTvZr	[46]	6.8	129.2	AC	S	BCC	C	RT	1473	215.9	
Mo0.7NbTv0.32r	[46]	7.1	139.4	AC	S	BCC	C	RT	1436	203.4	
Mo0.7NbTvZr	[46]	7.0	137.7	AC	S	BCC	C	RT	1706	245.5	
Mo1.3NbTv0.32r	[46]	7.4	164.2	AC	S	BCC	C	RT	1603	216.2	
Mo1.3NbTvZr	[46]	7.3	159.4	AC	S	BCC	C	RT	1496	205.5	
Mo1.5NbTv0.32r	[46]	7.5	171.0	AC	S	BCC	C	RT	1576	209.7	
Mo1.5NbTvZr	[46]	7.4		AC	M	2 BCC	C	RT	1603	217.3	
Mo1.7NbTvZr	[46]	7.5		AC	M	2 BCC	C	RT	1645	220.4	
Mo2NbTvZr	[46]	7.6		AC	M	2 BCC	C	RT	1765	232.6	

Monbiot <i>i</i> 0.25W	[47]	13.1	249.4	AC	S	BCC	C	RT	1109	84.7	
Monbiot <i>i</i> 0.5W	[47]	12.6	242.0	AC	S	BCC	C	RT	1211	96.1	
Monbiot <i>i</i> 0.75W	[47]	12.2	235.4	AC	S	BCC	C	RT	1304	107.3	
Monbiot <i>i</i> W	[48]	9.4	172.8	[58]/[39.2/48]	AC	S	BCC	C	RT	1400	149.4
Monbiot <i>i</i> W	[49]	11.0	212.5	(164.0)	AC	S	BCC	C	RT	1515	138.1
Monbiot <i>i</i> W	[49]	11.0		AC	S	BCC	C	RT	1200	659	
Monbiot <i>i</i> W	[49]	11.0		AC	S	BCC	C	RT	1000	752.8	
Monbiot <i>i</i> W	[49]	11.0		AC	S	BCC	C	RT	800	791.3	
Monbiot <i>i</i> W	[49]	11.0		AC	S	BCC	C	RT	600	973	
Monbiot <i>i</i> W	[47]	11.8	229.4	AC	S	BCC	C	RT	1455	123.8	
Monbiot <i>i</i> W	[49]	11.8	229.4	(156.0)	AC	S	BCC	C	RT	1343	
Monbiot <i>i</i> W	[49]	11.8		AC	S	BCC	C	RT	1200	586	
Monbiot <i>i</i> W	[49]	11.8		AC	S	BCC	C	RT	1000	620	
Monbiot <i>i</i> W	[49]	11.8		AC	S	BCC	C	RT	800	674	
Monbiot <i>i</i> W	[49]	11.8		AC	S	BCC	C	RT	600	689	
Monbiot <i>i</i> Zr	[50]	9.1		(153.0)	AC	M	2BCC	C	RT	1390	
Monbiot <i>i</i> Zr	[51]	9.1		AC	M	2BCC	C	RT	1375	150.5	
Monbiot <i>i</i> Zr	[51]	9.1		A	M	2BCC	C	RT	1100	120.4	
Monbiot <i>i</i> Zr	[52]	10.7	187.0	AC	S	BCC	C	RT	1525	142.7	
Monbiot <i>i</i> V	[53]	12.4	231.8	[19]/[218.0/58]	SPS	S	BCC	C	RT	2612	211.0
Monbiot <i>i</i> VW	[54]	12.4	231.8	[180.0]/204.5	HIP+A	S	BCC	C	RT	1246	100.7
Monbiot <i>i</i> VW	[54]	12.4		[19]/[218.0/58]	HIP+A	S	BCC	C	RT	1600	477
Monbiot <i>i</i> VW	[54]	12.4			HIP+A	S	BCC	C	RT	1400	656
Monbiot <i>i</i> VW	[54]	12.4			HIP+A	S	BCC	C	RT	1200	735
Monbiot <i>i</i> VW	[54]	12.4			HIP+A	S	BCC	C	RT	1000	842
Monbiot <i>i</i> VW	[54]	12.4			HIP+A	S	BCC	C	RT	800	846
Monbiot <i>i</i> VW	[54]	12.4			HIP+A	S	BCC	C	RT	600	862
Monbiot <i>i</i> W	[47]	13.7	257.8	228.7 [19]	AC	S	BCC	C	RT	996	72.9
Monbiot <i>i</i> W	[54]	13.7	257.8	(220.0)/228.7	HIP+A	S	BCC	C	RT	1058	77.5

		[19]							
MnNb ₂ W	[54]	13.7		HIP+IA	S	BCC	C	1600	405
MnNb ₂ W	[54]	13.7		HIP+IA	S	BCC	C	1400	421
MnNb ₂ W	[54]	13.7		HIP+IA	S	BCC	C	1200	506
MnNb ₂ W	[54]	13.7		HIP+IA	S	BCC	C	1000	548
MnNb ₂ W	[54]	13.7		HIP+IA	S	BCC	C	800	552
MnNb ₂ W	[54]	13.7		HIP+IA	S	BCC	C	600	561
MnNb ₂ TV	[3]	7.3	169.5	161.1 [57]	AC	S	BCC	C	RT
MnNb ₂ TV0.25Zr	[55]	7.3	152.9	141.6 [59]	AC	S	BCC	C	RT
MnNb ₂ TV0.32Zr	[46]	7.2	152.7		AC	S	BCC	C	RT
MnNb ₂ TV0.37Zr	[55]	7.2	151.6	141.7 [59]	AC	S	BCC	C	RT
MnNb ₂ TV0.5Zr	[55]	7.2	150.3	141.5 [59]	AC	S	BCC	C	RT
MnNb ₂ TV1.2Zr	[55]	7.1		AC	M	2 BCC	C	RT	1680
MnNb ₂ TV2Zr	[55]	7.0		AC	M	2 BCC	C	RT	1720
MnNb ₂ TV3Zr	[55]	6.9		AC	M	2 BCC	C	RT	1520
MnNb ₂ TV7Zr	[46]	7.1	149.2	139.5 [60]/141.1 [59]	AC	S	BCC	C	RT
MnNb ₂ TV12Zr	[55]	7.1	149.2	139.5 [60]/141.1 [59]	AC	S	BCC	C	RT
MnNb ₂ TiZr	[55]	7.3	154.5	140.1 [60]/141.7 [59]	AC	S	BCC	C	RT
MoTaIV	[6]	9.6	189.8		AC	S	BCC	C	RT
NbTaIV	[4]	9.2	133.8	(108.0)	AC	S	BCC	C	RT
NbTaIV	[56]	9.2	133.8		AC	S	BCC	C	RT
NbTaIVW	[56]	11.1	189.2	257.3 [58]	AC	S	BCC	C	RT
NbTaVN	[56]	12.9	207.5		AC	S	BCC	C	RT
NbTiIV3Zr	[46]	6.5	99.2		AC	S	BCC	C	RT
NbTiIV2Zr	[21]	6.4			HIP+IA	M	3 BCC	C	RT
NbTiIV2Zr	[21]	6.4			HIP+IA	M	3 BCC	C	1000
NbTiIV2Zr	[21]	6.4			HIP+IA	M	3 BCC	C	800
NbTiIV2Zr	[21]	6.4			HIP+IA	M	3 BCC	C	600
NbTiIV2Zr	[21]	6.5			HIP+IA	M	2 BCC	C	571
NbTiIV2Zr	[21]	6.5			HIP+IA	M	2 BCC	C	1105
NbTiIV2Zr	[21]	6.5			HIP+IA	M	2 BCC	C	1000
NbTiIV2Zr	[21]	6.5			HIP+IA	M	2 BCC	C	800
NbTiIV2Zr	[21]	6.5	104.3	[119.7 [60]/121.1 [59]]	AC	S	BCC	C	187
NbTiIV2Zr	[46]	6.5	104.3	[119.7 [60]/121.1 [59]]	AC	S	BCC	C	600
NbTiIV2Zr	[46]	6.5	104.3	[119.7 [60]/121.1 [59]]	AC	S	BCC	C	1104
NbTiIV2Zr	[46]	6.5	104.3	[119.7 [60]/121.1 [59]]	AC	S	BCC	C	170.9

with body centered cubic (BCC) structure. The results of 340 mechanical tests on 122 compositions are listed and then partially synthesized in graphical form for better visualization.

Table 1 of the data sheet illustrates the collected data from published studies so far [3–56], for all the RHEAs / RCCAs:

- the *alloy composition*. Alloying elements are classified by alphabetic order and the subscripts indicate atom mole fraction. A subscript of 1 is implied if none is shown.
- the *metallurgical state* of each tested alloy: non-equilibrium state such as-cast state, or optimized state via homogenization and annealing, thermally-processed conditions.
- the *phase content* present in the initial testing condition. From the mechanical properties point of view, it appears crucial, whether an alloy consists of a single phase, or of several phases.
- the *type of mechanical test*: tension or compression. Only mechanical tests with strain rates less than or equal to 10^{-3} s^{-1} are considered here.
- the *testing temperature*.
- The *experimental Young modulus*, when reported.
- the *yield strength* σ_y .

The *density* of each of the 122 compositions have been calculated on the basis of Rule of Mixtures (ROM) (Eq. 1):

$$\rho_{\text{alloy}} = \frac{\sum_{i=1}^N c_i A_i}{\sum_{i=1}^N c_i M_i} \quad (1)$$

Where c_i is the atomic fraction of element i in the alloy; A_i and M_i are the molar mass and molar volume of element i at room temperature. The *specific strength* is important for some structural applications. Therefore, such an important feature for structural part design, when available, is also listed in **Table 1**.

The *Young modulus* have also been estimated using ROM for single phase solid solutions (Eq. 2):

$$E_{\text{alloy}} = \sum_{i=1}^N x_i E_i \quad (2)$$

With x_i and E_i are the atomic fraction and the room temperature Young modulus of the alloy element i . Young modulus calculated from *ab initio* methods or determined experimentally are also provided in the table.

Acronyms used in **Table 1** represent:

RT: Room Temperature

ROM: Rule of Mixtures

AC: As-Cast

A: Annealed

HIP: Hot Isostatic Pressured

CR: Cold Rolled

SPS: Spark Plasma Sintering

SPD: Severe Plastic Deformation

T: Tension (tensile test)

C: Compression (compressive test)

It can be seen from **Table 1** of the data sheet that RHEAs and RCCAs have been studied over a wide temperature range between -268.8°C (4.2 K) and 1600°C (1873 K). For quick access and reading, a quantitative representation of the compiled data is illustrated in **Figs. 1** and **2**. This shows the evolution of yield strength and specific yield strength with temperature for a single phase or multiphase, multi-component alloys whatever the equilibrium condition/alloy processing.

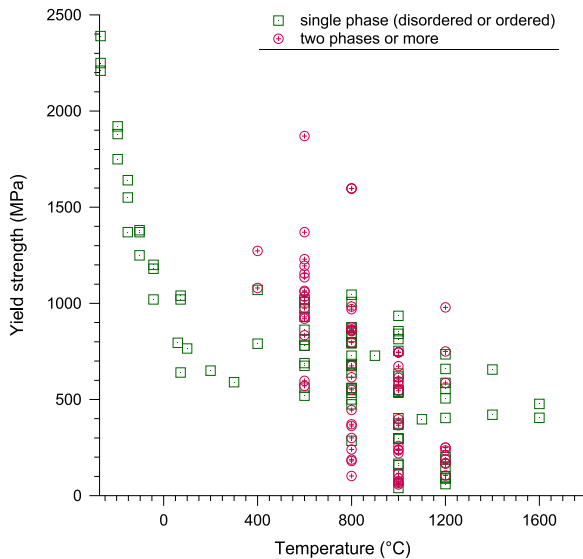


Fig. 1. Evolution of yield strength with temperature in the $-268.8\text{ }^{\circ}\text{C}$ – $1600\text{ }^{\circ}\text{C}$ range. For the sake of clarity all the collected data at room temperature have been excluded of this figure.

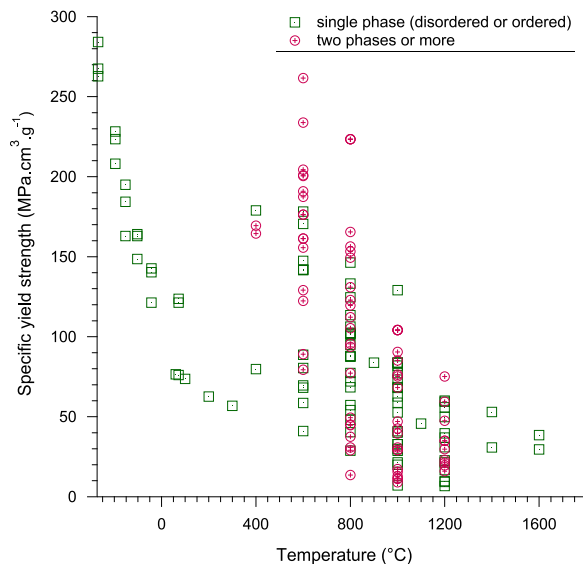


Fig. 2. Evolution of specific yield strength with temperature in the $-268.8\text{ }^{\circ}\text{C}$ – $1600\text{ }^{\circ}\text{C}$ range. For the sake of clarity all the collected data at room temperature have been excluded of this figure.

The data have been processed in order to directly visualize the evolution of mechanical properties with density, which could be very useful in the research for material solutions for applications at a given temperature. Figs. 3 and 4 display the evolution of yield stress with alloy density for the different multi-component at room temperature and $800\text{ }^{\circ}\text{C}$, respectively.

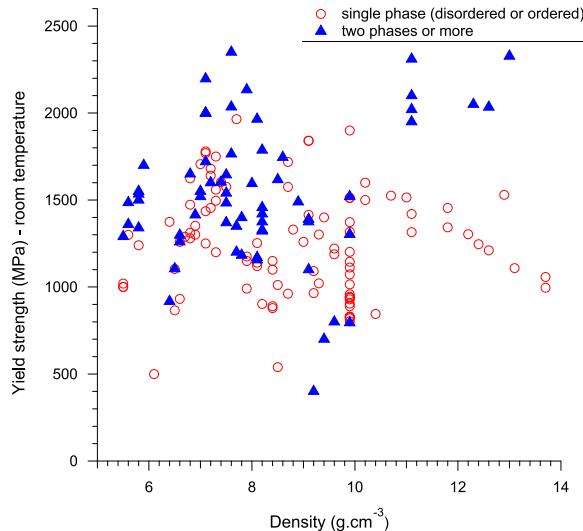


Fig. 3. Evolution of yield strength of RHEAs and RCCAs with alloy density at room temperature. Single and multi-phase alloys are distinguished.

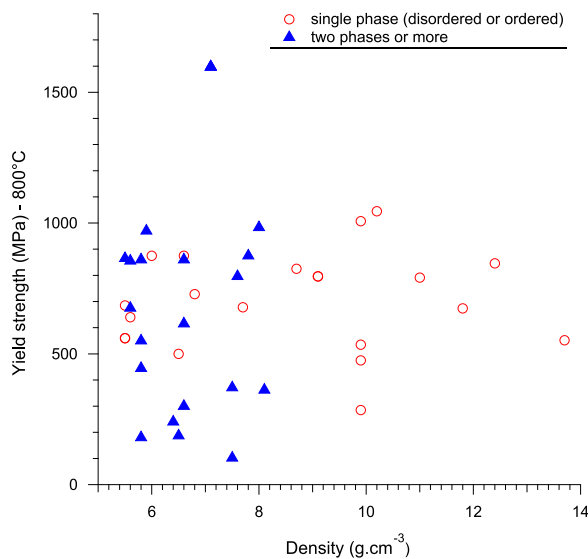


Fig. 4. Evolution of yield strength of RHEAs and RCCAs with alloy density at 800 °C. Single and multi-phase alloys are distinguished.

Acknowledgments

Work by O.N. Senkov was supported through the Air Force on-site contract FA8650-15-D-5230 managed by UES, Inc., Dayton, Ohio. J.-P. Couzinié and G. Dirras would like to gratefully acknowledge the French National Research Agency (ANR) for their support in the framework of the ANR 16-CE08-0027 “TURBO-AHEAD” program.

Transparency document. Supporting information

Transparency data associated with this article can be found in the online version at <https://doi.org/10.1016/j.dib.2018.10.071>.

References

- [1] O.N. Senkov, D.B. Miracle, K.J. Chaput, J.-P. Couzinie, Development and exploration of refractory high entropy alloys – a review, *J. Mater. Res.* 33 (2018) 3092–3128. <https://doi.org/10.1557/jmr.2018.153>.
- [2] S. Gorsse, D.B. Miracle, O.N. Senkov, Mapping the world of complex concentrated alloys, *Acta Mater.* 135 (2017) 177–187. <https://doi.org/10.1016/j.actamat.2017.06.027>.
- [3] S.Y. Chen, X. Yang, K.A. Dahmen, P.K. Liaw, Y. Zhang, Microstructures and crackling noise of Al_xNbTiMoV high entropy alloys, *Entropy* 16 (2014) 870–884. <https://doi.org/10.3390/e16020870>.
- [4] X. Yang, Y. Zhang, P.K. Liaw, Microstructure and Compressive Properties of NbTiVTaAlx High Entropy Alloys, in: C.M. Wang, C.J. Peng (Eds.), *Materials Science Forum*, 2012: pp. 292–298.
- [5] O.N. Senkov, J.K. Jensen, A.L. Pilchak, D.B. Miracle, H.L. Fraser, Compositional variation effects on the microstructure and properties of a refractory high-entropy superalloy AlMo_{0.5}NbTa_{0.5}TiZr, *Mater. Des.* 139 (2018) 498–511. <https://doi.org/10.1016/j.matdes.2017.11.033>.
- [6] D. Qiao, H. Jiang, X. Chang, Y. Lu, T. Li, Microstructure and mechanical properties of VTaTiMoAlx refractory high entropy alloys, *Mater. Sci. Forum* (2017) 638–642. <https://doi.org/10.4028/www.scientific.net/MSF.898.638>.
- [7] C.-M. Lin, C.-C. Juan, C.-H. Chang, C.-W. Tsai, J.-W. Yeh, Effect of Al addition on mechanical properties and microstructure of refractory Al_xHfNbTaTiZr alloys, *J. Alloy. Compd.* 624 (2015) 100–107. <https://doi.org/10.1016/j.jallcom.2014.11.064>.
- [8] O.N. Senkov, C. Woodward, D.B. Miracle, Microstructure and properties of aluminum-containing refractory high-entropy alloys, *JOM* 66 (2014) 2030–2042. <https://doi.org/10.1007/s11837-014-1066-0>.
- [9] O.N. Senkov, S.V. Senkova, C. Woodward, Effect of aluminum on the microstructure and properties of two refractory high-entropy alloys, *Acta Mater.* 68 (2014) 214–228. <https://doi.org/10.1016/j.actamat.2014.01.029>.
- [10] N.D. Stepanov, N.Y. Yurchenko, E.S. Panina, M.A. Tikhonovsky, S.V. Zhrebtssov, Precipitation-strengthened refractory Al_{0.5}CrNbTi₂V_{0.5} high entropy alloy, *Mater. Lett.* 188 (2017) 162–164. <https://doi.org/10.1016/j.matlet.2016.11.030>.
- [11] N.D. Stepanov, N.Y. Yurchenko, D.V. Skibin, M.A. Tikhonovsky, G.A. Salishchev, Structure and mechanical properties of the AlCr_xNbTi_{1-x} (x=0, 0.5, 1, 1.5) high entropy alloys, *J. Alloy. Compd.* 652 (2015) 266–280. <https://doi.org/10.1016/j.jallcom.2015.08.224>.
- [12] H. Chen, A. Kauffmann, B. Gorr, D. Schliephake, C. Seemueller, J.N. Wagner, H.-J. Christ, M. Heilmaier, Microstructure and mechanical properties at elevated temperatures of a new Al-containing refractory high-entropy alloy Nb-Mo-Cr-Ti-Al, *J. Alloy. Compd.* 661 (2016) 206–215. <https://doi.org/10.1016/j.jallcom.2015.11.050>.
- [13] H. Chen, A. Kauffmann, S. Laube, I.C. Choi, R. Schwaiger, K. Lichtenberg, F. Müller, B. Gorr, H.-J. Christ, M. Heilmaier, Contribution of lattice distortion to solid solution strengthening in a series of refractory high entropy alloys, *Mater. Trans. A-Phys. Metall. Mater. Sci.* (2017) 1–10. <https://doi.org/10.1007/s11661-017-4386-1>.
- [14] O.N. Senkov, D. Isheim, D.N. Seidman, A.L. Pilchak, Development of a refractory high entropy superalloy, *Entropy* (2016), <https://doi.org/10.3390/e18030102>.
- [15] N.D. Stepanov, D.G. Shaysultanov, G.A. Salishchev, M.A. Tikhonovsky, Structure and mechanical properties of a light-weight AlNbTi_{1-x} high entropy alloy, *Mater. Lett.* 142 (2015) 153–155. <https://doi.org/10.1016/j.matlet.2014.11.162>.
- [16] N.Y. Yurchenko, N.D. Stepanov, S.V. Zhrebtssov, M.A. Tikhonovsky, G.A. Salishchev, Structure and mechanical properties of B2 ordered refractory AlNbTi₂Zrx (x=0–1.5) high-entropy alloys, *Mater. Sci. Eng. A-Struct. Mater. Prop. Microstruct. Process.* 704 (2017) 82–90. <https://doi.org/10.1016/j.msea.2017.08.019>.
- [17] N.N. Guo, L. Wang, L.S. Luo, X.Z. Li, R.R. Chen, Y.Q. Su, J.J. Guo, H.Z. Fu, Microstructure and mechanical properties of in-situ MC-carbide particulates-reinforced refractory high-entropy Mo_{0.5}NbHf_{0.5}ZrTi matrix alloy composite, *Intermetallics* 69 (2016) 74–77. <https://doi.org/10.1016/j.intermet.2015.09.011>.
- [18] M. Zhang, X. Zhou, J. Li, Microstructure and mechanical properties of a refractory CoCrMoNbTi high-entropy alloy, *J. Mater. Eng. Perform.* 26 (2017) 3657–3665. <https://doi.org/10.1007/s11665-017-2799-z>.
- [19] E. Fazakas, V. Zadorozhny, L.K. Varga, A. Inoue, D.V. Louzguine-Luzgin, F. Tian, L. Vitos, Experimental and theoretical study of Ti₂₀Zr₂₀Hf₂₀Nb₂₀X₂₀ (X = V or Cr) refractory high-entropy alloys, *Int. J. Refract. Met. Hard Mater.* 47 (2014) 131–138. <https://doi.org/10.1016/j.ijrmhm.2014.07.009>.
- [20] O.N. Senkov, C.F. Woodward, Microstructure and properties of a refractory NbCrMo_{0.5}Ta_{0.5}TiZr alloy, *Mater. Sci. Eng. A-Struct. Mater. Prop. Microstruct. Process.* 529 (2011) 311–320. <https://doi.org/10.1016/j.msea.2011.09.033>.
- [21] O.N. Senkov, S.V. Senkova, D.B. Miracle, C. Woodward, Mechanical properties of low-density, refractory multi-principal element alloys of the Cr-Nb-Ti-V-Zr system, *Mater. Sci. Eng. A-Struct. Mater. Prop. Microstruct. Process.* 565 (2013) 51–62. <https://doi.org/10.1016/j.msea.2012.12.018>.
- [22] O.A. Waseem, J. Lee, H.M. Lee, H.J. Ryu, The effect of Ti on the sintering and mechanical properties of refractory high-entropy alloy Ti_xWTaVCr fabricated via spark plasma sintering for fusion plasma-facing materials, *Mater. Chem. Phys.* (2017), <https://doi.org/10.1016/j.matchemphys.2017.06.054>.
- [23] M. Feuerbacher, M. Heidelmann, C. Thomas, Plastic deformation properties of Zr-Nb-Ti-Ta-Hf high-entropy alloys, *Philos. Mag.* 95 (2015) 1221–1232. <https://doi.org/10.1080/14786435.2015.1028506>.
- [24] N.N. Guo, L. Wang, L.S. Luo, X.Z. Li, R.R. Chen, Y.Q. Su, J.J. Guo, H.Z. Fu, Microstructure and mechanical properties of refractory high entropy (Mo_{0.5}NbHf_{0.5}ZrTi)(BCC)/M₅Si₃ in-situ compound, *J. Alloy. Compd.* 660 (2016) 197–203. <https://doi.org/10.1016/j.jallcom.2015.11.091>.

- [25] S. Sheikh, S. Shafeie, Q. Hu, J. Ahlstrom, C. Persson, J. Vesely, J. Zylka, U. Klement, S. Guo, Alloy design for intrinsically ductile refractory high-entropy alloys, *J. Appl. Phys.* 120 (2016) 164902. <https://doi.org/10.1063/1.4966659>.
- [26] A.V. Podolskiy, E.D. Tabachnikova, V.V. Voloschuk, V.F. Gorban, N.A. Krapivka, S.A. Firstov, Mechanical properties and thermally activated plasticity of the Ti₃₀Zr₂₅Hf₁₅Nb₂₀Ta₁₀ high entropy alloy at temperatures 4.2–350 K, *Mater. Sci. Eng. A-Struct. Mater. Prop. Microstruct. Process.* 710 (2018) 136–141. <https://doi.org/10.1016/j.msea.2017.10.073>.
- [27] C.-C. Juan, K.-K. Tseng, W.-L. Hsu, M.-H. Tsai, C.-W. Tsai, C.-M. Lin, S.-K. Chen, S.-J. Lin, J.-W. Yeh, Solution strengthening of ductile refractory HfMoNbTaTiZr high-entropy alloys, *Mater. Lett.* 175 (2016) 284–287. <https://doi.org/10.1016/j.matlet.2016.03.133>.
- [28] Y. Liu, Y. Zhang, H. Zhang, N. Wang, X. Chen, H. Zhang, Y. Li, Microstructure and mechanical properties of refractory HfMoO_{0.5}NbTiV_{0.5}Six high-entropy composites, *J. Alloy. Compd.* 694 (2017) 869–876. <https://doi.org/10.1016/j.jallcom.2016.10.014>.
- [29] C.-C. Juan, M.-H. Tsai, C.-W. Tsai, C.-M. Lin, W.-R. Wang, C.-C. Yang, S.-K. Chen, S.-J. Lin, J.-W. Yeh, Enhanced mechanical properties of HfMoTaTiZr and HfMoNbTaTiZr refractory high-entropy alloys, *Intermetallics* 62 (2015) 76–83. <https://doi.org/10.1016/j.intermet.2015.03.013>.
- [30] N.N. Guo, L. Wang, L.S. Luo, X.Z. Li, Y.Q. Su, J.J. Guo, H.Z. Fu, Microstructure and mechanical properties of refractory MoNbHfZrTi high-entropy alloy, *Mater. Des.* 81 (2015) 87–94. <https://doi.org/10.1016/j.matdes.2015.05.019>.
- [31] L. Lilensten, J.-P. Couzinié, J. Bourgon, L. Perriere, G. Dirras, F. Prima, I. Guillot, Design and tensile properties of a bcc Ti-rich high-entropy alloy with transformation-induced plasticity, *Mater. Res. Lett.* 5 (2017) 110–116. <https://doi.org/10.1080/21663831.2016.1221861>.
- [32] Y. Zhang, Y. Liu, Y. Li, X. Chen, H. Zhang, Microstructure and mechanical properties of a refractory HfNbTiVSi0.5 high-entropy alloy composite, *Mater. Lett.* 174 (2016) 82–85. <https://doi.org/10.1016/j.matlet.2016.03.092>.
- [33] Y. Zhang, Y. Liu, Y. Li, X. Chen, H. Zhang, Microstructure and mechanical properties of a new refractory HfNbSi0.5TiVZr high entropy alloy, *Mater. Sci. Forum* (2016) 76–84. <https://doi.org/10.4028/www.scientific.net/MSF.849.76>.
- [34] B. Schuh, B. Voelker, J. Todt, N. Schell, L. Perriere, J. Li, J.-P. Couzinié, A. Hohenwarter, Thermodynamic instability of a nanocrystalline, single-phase Ti₂ZrNbHfTa alloy and its impact on the mechanical properties, *Acta Mater.* 142 (2018) 201–212. <https://doi.org/10.1016/j.actamat.2017.09.035>.
- [35] O.N. Senkov, S.L. Semiatin, Microstructure and properties of a refractory high-entropy alloy after cold working, *J. Alloy. Compd.* 649 (2015) 1110–1123. <https://doi.org/10.1016/j.jallcom.2015.07.209>.
- [36] C.-C. Juan, M.-H. Tsai, C.-W. Tsai, W.-L. Hsu, C.-M. Lin, S.-K. Chen, S.-J. Lin, J.-W. Yeh, Simultaneously increasing the strength and ductility of a refractory high-entropy alloy via grain refining, *Mater. Lett.* 184 (2016) 200–203. <https://doi.org/10.1016/j.matlet.2016.08.060>.
- [37] L. Lilensten, J.-P. Couzinié, L. Perriere, A. Hocini, C. Keller, G. Dirras, I. Guillot, Study of a bcc multi-principal element alloy: tensile and simple shear properties and underlying deformation mechanisms, *Acta Mater.* 142 (2018) 131–141. <https://doi.org/10.1016/j.actamat.2017.09.062>.
- [38] O.N. Senkov, J.M. Scott, S.V. Senkova, D.B. Miracle, C.F. Woodward, Microstructure and room temperature properties of a high-entropy TaNbHfZrTi alloy, *J. Alloy. Compd.* 509 (2011) 6043–6048. <https://doi.org/10.1016/j.jallcom.2011.02.171>.
- [39] J.-P. Couzinié, L. Lilensten, Y. Champion, G. Dirras, L. Perriere, I. Guillot, On the room temperature deformation mechanisms of a Ti₂ZrHfNbTa refractory high-entropy alloy, *Mater. Sci. Eng. A-Struct. Mater. Prop. Microstruct. Process.* 645 (2015) 255–263. <https://doi.org/10.1016/j.msea.2015.08.024>.
- [40] G. Dirras, H. Couque, L. Lilensten, A. Heczel, D. Tingaud, J.-P. Couzinié, L. Perriere, J. Gubicza, I. Guillot, Mechanical behavior and microstructure of Ti₂₀Hf₂₀Zr₂₀Ta₂₀Nb₂₀ high-entropy alloy loaded under quasi-static and dynamic compression conditions, *Mater. Charact.* 111 (2016) 106–113. <https://doi.org/10.1016/j.matchar.2015.11.018>.
- [41] G. Dirras, L. Lilensten, P. Djemnia, M. Laurent-Brocq, D. Tingaud, J.-P. Couzinié, L. Perriere, T. Chauveau, I. Guillot, Elastic and plastic properties of as-cast equimolar TiHfZrTaNb high-entropy alloy, *Mater. Sci. Eng. A-Struct. Mater. Prop. Microstruct. Process.* 654 (2016) 30–38. <https://doi.org/10.1016/j.msea.2015.12.017>.
- [42] O.N. Senkov, J.M. Scott, S.V. Senkova, F. Meisenkothen, D.B. Miracle, C.F. Woodward, Microstructure and elevated temperature properties of a refractory TaNbHfZrTi alloy, *J. Mater. Sci.* 47 (2012) 4062–4074. <https://doi.org/10.1007/s10853-012-6260-2>.
- [43] S. Maiti, W. Steurer, Structural-disorder and its effect on mechanical properties in single-phase TaNbHfZr high-entropy alloy, *Acta Mater.* 106 (2016) 87–97. <https://doi.org/10.1016/j.actamat.2016.01.018>.
- [44] Y.D. Wu, Y.H. Cai, T. Wang, J.J. Si, J. Zhu, Y.D. Wang, X.D. Hui, A refractory Hf₂₅Nb₂₅Ti₂₅Zr₂₅ high-entropy alloy with excellent structural stability and tensile properties, *Mater. Lett.* 130 (2014) 277–280. <https://doi.org/10.1016/j.matlet.2014.05.134>.
- [45] H. Huang, Y. Wu, J. He, H. Wang, X. Liu, K. An, W. Wu, Z. Lu, Phase-transformation ductilization of brittle high-entropy alloys via metastability engineering, *Adv. Mater.* 29 (2017) 1701678. <https://doi.org/10.1002/adma.201701678>.
- [46] Y.D. Wu, Y.H. Cai, X.H. Chen, T. Wang, J.J. Si, L. Wang, Y.D. Wang, X.D. Hui, Phase composition and solid solution strengthening effect in Ti₂ZrNbMoV high-entropy alloys, *Mater. Des.* 83 (2015) 651–660. <https://doi.org/10.1016/j.matdes.2015.06.072>.
- [47] Z.D. Han, H.W. Luan, X. Liu, N. Chen, X.Y. Li, Y. Shao, K.F. Yao, Microstructures and mechanical properties of Ti_xNbMoTaW refractory high-entropy alloys, *Mater. Sci. Eng. A-Struct. Mater. Prop. Microstruct. Process.* 712 (2017) 380–385. <https://doi.org/10.1016/j.msea.2017.12.004>.
- [48] H.W. Yao, J.W. Qiao, J.A. Hawk, H.F. Zhou, M.W. Chen, M.C. Gao, Mechanical properties of refractory high-entropy alloys: experiments and modeling, *J. Alloy. Compd.* 696 (2017) 1139–1150. <https://doi.org/10.1016/j.jallcom.2016.11.188>.
- [49] Z.D. Han, N. Chen, S.F. Zhao, L.W. Fan, G.N. Yang, Y. Shao, K.F. Yao, Effect of Ti additions on mechanical properties of NbMoTaW and VNbMoTaW refractory high entropy alloys, *Intermetallics* 84 (2017) 153–157. <https://doi.org/10.1016/j.intermet.2017.01.007>.
- [50] S.-P. Wang, J. Xu, Ti₂ZrNbTaMo high-entropy alloy designed for orthopedic implants: as-cast microstructure and mechanical properties, *Mater. Sci. Eng. C-Mater. Biol. Appl.* 73 (2017) 80–89. <https://doi.org/10.1016/j.msec.2016.12.057>.
- [51] M. Todai, T. Nagase, T. Hori, A. Matsugaki, A. Sekita, T. Nakano, Novel TiNbTaZrMo high-entropy alloys for metallic biomaterials, *Scr. Mater.* 129 (2017) 65–68. <https://doi.org/10.1016/j.scriptamat.2016.10.028>.

- [52] H. Yao, J.-W. Qiao, M.C. Gao, J.A. Hawk, S.-G. Ma, H. Zhou, MoNbTaV medium-entropy alloy, Entropy 18 (2016) 189. <https://doi.org/10.3390/e18050189>.
- [53] B. Kang, J. Lee, H.J. Ryu, S.H. Hong, Ultra-high strength WNbMoTaV high-entropy alloys with fine grain structure fabricated by powder metallurgical process, Mater. Sci. Eng. A-Struct. Mater. Prop. Microstruct. Process. 712 (2018) 616–624. <https://doi.org/10.1016/j.msea.2017.12.021>.
- [54] O.N. Senkov, G.B. Wilks, J.M. Scott, D.B. Miracle, Mechanical properties of Nb25Mo25Ta25W25 and V20Nb20Mo20-Ta20W20 refractory high entropy alloys, Intermetallics 19 (2011) 698–706. <https://doi.org/10.1016/j.intermet.2011.01.004>.
- [55] Y. Zhang, X. Yang, P.K. Liaw, Alloy design and properties optimization of high-entropy alloys, JOM 64 (2012) 830–838. <https://doi.org/10.1007/s11837-012-0366-5>.
- [56] H.W. Yao, J.W. Qiao, M.C. Gao, J.A. Hawk, S.G. Ma, H.F. Zhou, Y. Zhang, NbTaV-(Ti,W) refractory high-entropy alloys: experiments and modeling, Mater. Sci. Eng. A-Struct. Mater. Prop. Microstruct. Process. 674 (2016) 203–211. <https://doi.org/10.1016/j.msea.2016.07.102>.
- [57] P. Cao, X. Ni, F. Tian, L.K. Varga, L. Vitos, Ab initio study of AlxMoNbTiV high-entropy alloys, J. Phys.-Condens. Matter 27 (2015) 075401. <https://doi.org/10.1088/0953-8984/27/7/075401>.
- [58] S.-M. Zheng, W.-Q. Feng, S.-Q. Wang, Elastic properties of high entropy alloys by MaxEnt approach, Comput. Mater. Sci. 142 (2018) 332–337. <https://doi.org/10.1016/j.commatsci.2017.09.060>.
- [59] F. Tian, L.K. Varga, N. Chen, J. Shen, L. Vitos, Ab initio design of elastically isotropic TiZrNbMoVx high-entropy alloys, J. Alloy. Compd. 599 (2014) 19–25. <https://doi.org/10.1016/j.jallcom.2014.01.237>.
- [60] L.-Y. Tian, G. Wang, J.S. Harris, D.L. Irving, J. Zhao, L. Vitos, Alloying effect on the elastic properties of refractory high-entropy alloys, Mater. Des. 114 (2017) 243–252. <https://doi.org/10.1016/j.matdes.2016.11.079>.